VIII. 1. Imaging of Hypoxic Tissues in Glioblastoma by PET with [^{18}F]FRP-170, a New ^{18}F-labeled 2-Nitroimidazole Analog

Shibahara I.[1], Kumabe T.[1], Kanamori M.[1], Saito R.[1], Sonoda Y.[1], Watanabe M.[2], Iwata R.[3], Tashiro M.[3], Takanami K.[4], Kaneta T.[4], Takai Y.[5], Fukuda H.[6], and Tominaga T.[1]

Departments of [1]Neurosurgery[2], Pathology, and [4]Diagnostic Radiology, Tohoku University Graduate School of Medicine
[3]Cyclotron and Radioisotope Center, Tohoku University
[5]Department of Radiology, Hirosaki University School of Medicine & Hospital
[6]Department of Nuclear Medicine and Radiology, Institute of Development, Aging and Cancer, Tohoku University

Introduction

Tumor hypoxia arises in solid cancer tissues with inadequate supply of oxygen, and may be important in clinical diagnosis because hypoxia may determine tumor aggressiveness and treatment response[1,2], which are both essential information for treatment selection. The presence of hypoxic condition within brain tumors was confirmed using tube-type pO_2 sensors[3]. The mean intratumoral pO_2 value was 15.3±2.3 mmHg, and pO_2 in brain tissue around the tumor was 59.8±6.5 mmHg. However, these sensing methods are rather invasive, limiting the accessible tumor sites, and not easily applicable for routine clinical usage. A series of 2-nitroimidazoles have been developed as selective radiosensitizers of hypoxic cells, based on the property of selective accumulation and retention in hypoxic cells until the cells die[4]. Therefore, radiolabeled 2-nitroimidazoles have been developed for the direct visualization of tissue hypoxia in tumors[5].

^{18}F-fluoromisonidazole ([^{18}F]FMISO) was the first such radiopharmaceutical developed[6,7], and [^{18}F]FMISO positron emission tomography (PET) has been used to detect hypoxic areas in glioblastoma[8-10]. However, FMISO has failed to gain wider acceptance for routine clinical application because of various limitations, such as slow accumulation in hypoxic tumors, low target-to-background contrast, and significant amounts of radioactive metabolic products. Misonidazole is rather lipophilic, whereas high hydrophilicity is thought to be better for imaging hypoxia because of rapid blood clearance and high

target-to-background ratio. Many 2-nitroimidazole analogs have been developed by modifying the side chain, such as etanidazole with an octanol-water partition coefficient (p value) of 0.046[11]. Fluoroetanidazole (FETA) also has a lower p value (0.16)[12] than FMISO (0.40), so the levels of retention of [^{18}F]FETA in the liver and lung are significantly lower than those of [^{18}F]FMISO[13]. [^{18}F]fluoroerythronitroimidazole and [^{18}F]fluoroazomycin arabinoside have also been developed as hydrophilic hypoxia markers, with lower p value and better tumor-to-blood ratio than [^{18}F]FMISO[14,15].

RP170, 1-(2-hydroxy-1-[hydroxymethyl]ethoxy)methyl-2-nitroimidazole, a 2-nitroimidazole analog with a hydrophilic side chain has a p value of 0.094, much lower than that of misonidazole[16-18]. Recently, a new hypoxia imaging compound, 1-(2-fluoro-1-[hydroxylmethyl]ethoxy)methyl-2-nitroimidazole or [^{18}F]FRP-170, was developed for clinical PET imaging, which is expected to show improvements over [^{18}F]FMISO with regard to higher image contrast and faster clearance[19-21]. Hypoxic lesions of murine tumors, ischemic myocardium of rats, and hypoxic lesions in lung cancer patients have been visualized using this compound[19,20,22].

Here we describe the demonstration of hypoxic tissues in a patient with glioblastoma resistant to radiochemotherapy using [^{18}F]FRP-170 PET, and confirmed the mechanism of radioresistance as the induction of hypoxia-inducible factor 1 (HIF1)-alpha.

Materials and Methods

This study was conducted with the approval of the Ethics Committee of Tohoku University School of Medicine, and written informed consent was obtained from all participants. Three patients, a 53-year-old male with glioblastoma, a 68-year-old male with glioblastoma, and a 53-year-old female with oligodendroglioma, underwent [^{18}F]FRP-170 PET imaging and tissue specimens were obtained by biopsy or surgery.

[^{18}F]FRP-170 was prepared with an automated synthesizer using an on-column basic hydrolysis step as reported previously[23]. The overall radiochemical yield was around 20–30% (decay-corrected) with specific activity of >26 GBq/μmol within 60 minutes. The PET scans for patients were performed 120 minutes after intravenous bolus injection of about 370 MBq of [^{18}F]FRP-170 using a PET scanner (ECAT EXACT HR+; Siemens). Maximum standardized uptake values (SUVmax) were obtained by drawing regions of interest on the PET images covering the tumor and reference tissue in the contralateral normal hemisphere and posterior cervical muscle region.

The tissue specimens were examined by the same neuropathologist (M.W.) and the diagnosis was based on the classification of the World Health Organization[24]. All surgical specimens were examined for the detection of hypoxic tissues. Formalin-fixed, paraffin-embedded tumor tissue was cut into 2 μm sections and mounted on saline-coated slides. After deparaffinization, washing and blocking processes, the sections were incubated with goat polyclonal primary antibody of HIF1-alpha (Santa Cruz Biotechnology, Santa Cruz, CA), which was diluted 1:100, overnight at 4 degrees centigrade. Then sections were washed in phosphate buffered saline, and incubated with biotinylated anti-goat immunoglobulin G diluted 1:100 for 30 minutes at room temperature. Positive immunostaining for HIF1-alpha was judged as brown staining of the cytoplasm.

Illustrative Case

A 53-year-old male, who had previously been healthy, suddenly screamed meaningless words and lost consciousness for 5 minutes. A similar episode happened on the following night, so his family took him to a nearby emergency unit. On admission, he was slightly disoriented with motor aphasia. Computed tomography of the head revealed an edematous lesion in the left hemisphere with midline shift to the right (Fig. 1A). Magnetic resonance (MR) imaging of the head with gadolinium revealed a hypointense lesion mainly in the left insula with spotty enhancement (Fig. 1B). The episodes of the past two nights were diagnosed as symptomatic seizure, and 200 mg of zonisamide per day was prescribed.

The patient underwent a stereotactic needle biopsy, and the histological diagnosis was glioblastoma. He was treated with 60 Gy of radiation therapy combined with intravenous administration of nimustine hydrochloride. However, the tumor kept growing (Fig. 1C). Therefore, he underwent left osteoplastic fronto-temporal craniotomy and partial removal of the tumor. To avoid right hemiparesis, the medial part of tumor involving the left lateral lenticulostriate arteries was not resected (Fig. 1D). Follow-up MR imaging with gadolinium obtained 4 weeks after the surgery revealed progression of the tumor, and [^{18}F]FRP-170 PET showed a marked hypoxic lesion corresponding to the enhanced lesion on MR imaging (Fig. 2A, B). He underwent additional 27 Gy of booster irradiation localized to the enhanced lesion with oral administration of temozolomide. However, follow-up MR imaging revealed further progression of the tumor. Clinical examination showed right hemiparesis and aphasia. The patient was discharged for the best supportive care.

Results

[^{18}F]FRP-170 PET detected hypoxic lesion as high intensity areas, and the relative intensity was calculated by comparison with the control areas. In the illustrative case, the SUVmax values for tumor tissue and posterior cervical muscle were 1.6 and 1.0, respectively (Fig. 2B). The tumor/muscle (T/M) ratio was calculated as 1.6. This indicates that tumor cells were located in the hypoxic lesion. Immunostaining with HIF1-alpha antibody of the tissue obtained from the surgery showed many positive cells, with brown staining of the cytoplasm, indicating induction of HIF1-alpha protein and the presence of hypoxic condition within the tumor (Fig. 3B). Interestingly, the number of HIF1-alpha-positive cells increased in the second specimen obtained from the surgery after 60 Gy of radiation therapy (Fig. 3B) compared to the first tissue specimen from the initial biopsy (Fig. 3A).

In the second patient, a 68-year-old male with glioblastoma (Fig. 4A), SUVmax was 2.3 and T/M ratio was 2.3 (Fig. 4B), indicating the presence of marked hypoxic tissue. In the third patient, a 53-year-old female with oligodendroglioma (Fig. 4D), SUVmax was 1.3 and T/M ratio was 1.2 (Fig. 4E), indicating almost no hypoxic condition within the tumor. In accordance with the PET findings, immunostaining for HIF1-alpha showed many positive cells in the second patient with glioblastoma (Fig. 4C) and almost no positive cells in the third patient with oligodendroglioma (Fig. 4F).

Discussion

The present study showed that [^{18}F]FRP-170 PET could visualize hypoxic lesions in two glioblastoma patients, which were histologically confirmed as hypoxia by upregulation of HIF1-alpha protein (Figs. 3B and 4C), and demonstrated the absence of hypoxia in a patient with oligodendroglioma (Fig. 4E, F). The illustrative case had strong resistance to radiochemotherapy, suggesting that the hypoxic condition might be involved.

Assessment of the hypoxic condition within a tumor is useful to estimate the tumor aggressiveness[25] and prognosis[26] and select the optimum therapy. Pretreatment with nitroglycerin decreased hypoxia-induced resistance to anticancer drugs in lung adenocarcinoma patients[27], and the mechanism involved downregulation of HIF1-alpha[28]. Moreover, inhibition of HIF1-alpha in combination with temozolomide had robust antitumor efficacy in the *in vivo* glioma xenograft model[29]. Therefore, if the degree of hypoxia can be assessed noninvasively, we can take appropriate action to reduce the

hypoxia-induced resistance through downregulation of HIF1-alpha. We may be able to offer more aggressive therapy to patients with poor prognosis, which cannot be accepted for most patients due to the increased side effects[26].

Expression of HIF1-alpha was strong in 12 of 51 cases of oligodendroglioma, moderate in 21, weak in 8, and none in 10[30]. Our case of oligodendroglioma showed no HIF1-alpha immunostaining, possibly because this case was categorized in weak or none subgroup. HIF1-alpha expression correlates to increased risk of treatment failure and death in patients with breast and cervical cancers, despite the low tumor grade[26]. If this is also true in glioma, applying this imaging to glioma patients may be very important for treatment selection.

A significant difference was detected in the positive rate of HIF1-alpha immunostaining between the first and second tumor tissues obtained in the illustrative case (Fig. 3A, B). The patient was treated with 60 Gy of radiation therapy with nimustine hydrochloride between these two time points. Radiosensitive cells and/or cells in normoxia may have been eradicated by such treatments, whereas unresponsive cells or cells in hypoxia may have survived. This finding suggests that both the histopathology and hypoxic condition are important factors for treatment sensitivity.

Conclusion

[^{18}F]FRP-170 PET could visualize the hypoxic tissues within glioblastoma with relatively high T/M ratio, as confirmed by HIF1-alpha immunohistochemistry. Such findings can provide noninvasive indications of the aggressiveness and prognosis of glioma.

References

1) Brizel D.M., Dodge R.K., Clough R.W., Dewhirst M.W., Radiother Oncol. **53** (1999) 113.
2) Brown J.M., Int. J. Radiat. Oncol. Biol. Phys. **49** (2001) 319.
3) Kayama T., Yoshimoto T., Fujimoto S., Sakurai Y., J. Neurosurg. **74** (1991) 55.
4) Nunn A., Linder K., Strauss H.W., Eur. J. Nucl. Med. **22** (1995) 265.
5) Chapman J., Franko A., Sharplin J., Br. J. Cancer **43** (1981) 546.
6) Jerabek P.A., Patrick T.B., Kilbourn M.R., Dischino D.D., Welch M.J., Int. J. Rad. Appl. Instrum. **A37** (1986) 599.
7) Martin G.V., Caldwell J.H., Graham M.M., Grierson J.R., Kroll K., Cowan M.J., et al., J. Nucl. Med. **33** (1992) 2202.
8) Cher L.M., Murone C., Lawrentschuk N., Ramdave S., Papenfuss A., Hannah A., et al., J. Nucl. Med. **47** (2006) 410.
9) Spence A.M., Muzi M., Swanson K.R., O'Sullivan F., Rockhill J.K., Rajendran J.G., et al., Clin. Cancer Res. **14** (2008) 2623.
10) Tochon-Danguy H.J., Sachinidis J.I., Chan F., Chan J.G., Hall C., Cher L., et al., Nucl. Med. Biol. **29** (2002) 191.
11) Brown J.M., Workman P., Radiat. Res. **82** (1980) 171.

12) Barthel H., Wilson H., Collingridge D.R., Brown G., Osman S., Luthra S.K., et al., Br. J. Cancer **90** (2004) 2232.13) Rasey J.S., Hofstrand P.D., Chin L.K., Tewson T.J., J. Nucl. Med. **40** (1999) 1072.
13) Rasey J.S., Hofstrand P.D., Chin L.K., Tewson T.J., J. Nucl. Med. **40** (1999) 1072.
14) Kumar P., Stypinski D., Xia H., McEwan A., Machulla H., Wiebe L.I., J. Labelled. Comp. Radiopharm. **42** (1999) 3.
15) Yang D.J., Wallace S., Cherif A., Li C., Gretzer M.B., Kim E.E., et al., Radiology **194** (1995) 795.
16) Murayama C., Suzuki A., Sato C., Tanabe Y., Miyata Y., Shoji T., et al., Int. J. Radiat. Oncol. Biol. Phys. **22** (1992) 557.
17) Murayama C., Suzuki A., Suzuki T., Miyata Y., Sakaguchi M., Tanabe Y., et al., Int. J. Radiat. Oncol. Biol. Phys. **17** (1989) 575.
18) Sasai K., Shibamoto Y., Takahashi M., Abe M., Wang J., Zhou L., et al., Jpn. J. Cancer Res. **80** (1989) 1113.
19) Kaneta T., Takai Y., Iwata R., Hakamatsuka T., Yasuda H., Nakayama K., et al., Ann. Nucl. Med. **21** (2007) 101.
20) Kaneta T., Takai Y., Kagaya Y., Yamane Y., Wada H., Yuki M., et al., J. Nucl. Med. **43** (2002) 109.
21) Wada H., Iwata R., Ido T., Takai Y., J. Labelled. Comp. Radiopharm. **43** (2000) 785.
22) Takai Y., Kaneta T., Hakamatsuka T., Nemoto K., Ogawa Y., Yamada S., et al., Int. J. Radiat. Oncol. Biol. Phys. **63** (Suppl) (2005) S465-S466.
23) Ishikawa Y., Iwata R., Furumoto S., Takai Y., Appl. Radiat. Isot. **62** (2005) 705.
24) Louis D.N., Ohgaki H., Wiestler O.D., Cavenee W.K., Burger P.C., Jouvet A., et al., (eds) Lyon: IARC, 2007.
25) Evans S.M., Judy K.D., Dunphy I., Jenkins W.T., Hwang W.T., Nelson P.T., et al., Clin. Cancer Res. **10** (2004) 8177.
26) Semenza G.L., Trends Mol. Med. **8** (4 Suppl) (2002) S62-67.
27) Yasuda H., Nakayama K., Watanabe M., Suzuki S., Fuji H., Okinaga S., et al., Clin. Cancer Res. **12** (2006) 6748.
28) Huang L.E., Willmore W.G., Gu J., Goldberg M.A., Bunn H.F., J. Biol. Chem. **274** (1999) 9038.
29) Li L., Lin X., Shoemaker A.R., Albert D.H., Fesik S.W., Shen Y., Clin. Cancer. Res. **12** (2006) 4747.
30) Birner P., Gatterbauer B., Oberhuber G., Schindl M., Rossler K., Prodinger A., et al., Cancer **92** (2001) 165.

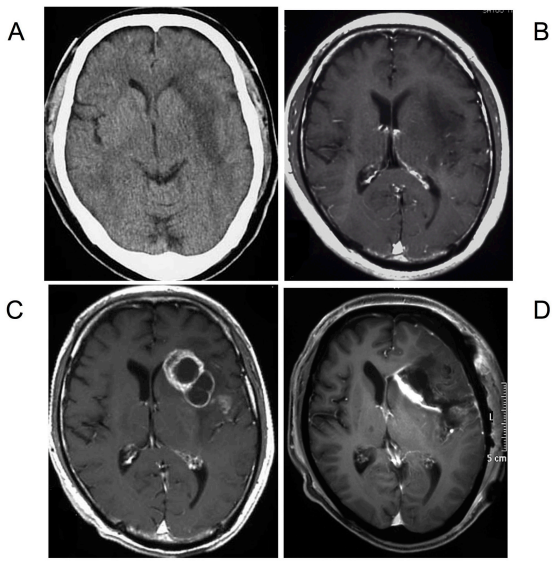

Figure 1. Illustrative case. Axial computed tomography scan (A) and T1-weighted magnetic resonance (MR) image with gadolinium (B) on admission, showing a diffuse infiltrative tumor in the left insulo-opercular region. Axial T1-weighted MR image with gadolinium after 60 Gy of irradiation (C), demonstrating tumor progression. Axial T1-weighted MR image with gadolinium after surgery (D), depicting partial resection of the tumor.

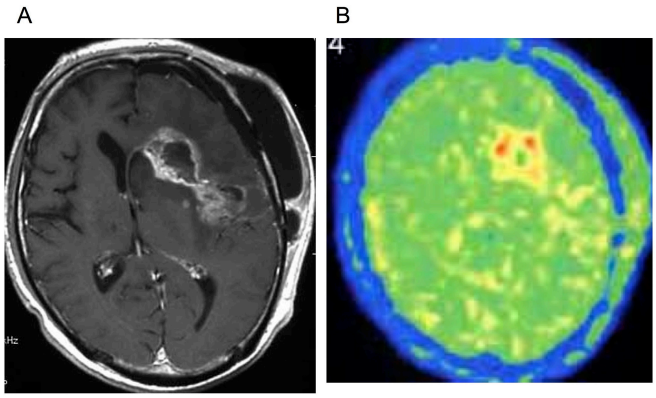

Figure 2. Illustrative case. Axial T1-weighted MR image with gadolinium obtained 4 weeks after the surgery (A), demonstrating further progression of the tumor. [^{18}F]FRP-170 positron emission tomography (PET) image(B), depicting high uptake corresponding to the enhanced lesion on MR imaging.

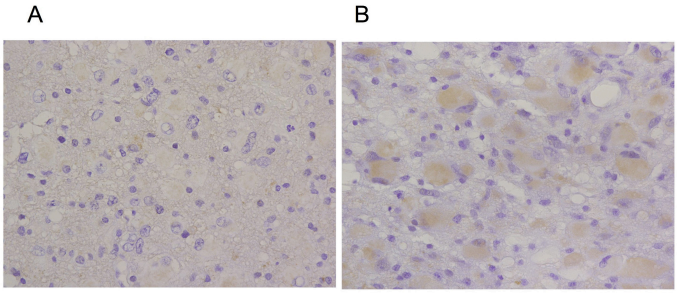

Figure 3. Photomicrographs of the glioblastoma from the illustrative case. HIF1-alpha-positive cells can be seen as brown staining of cytoplasm. The first tissue from the stereotactic biopsy contains fewer positive cells (A) compared to the second tissue from the surgery, which was performed after 60 Gy of irradiation with chemotherapy (B) (original magnificationx400).

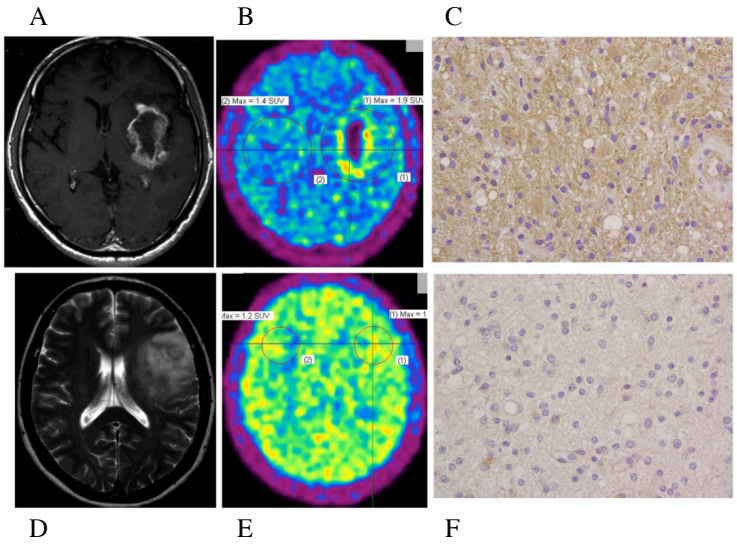

Figure 4. Axial T1-weighted MR image with gadolinium from a 68-year-old male with glioblastoma, showing an enhanced lesion in the left insula (A). [^{18}F]FRP-170 PET image showing high uptake (B), corresponding to the enhanced lesion on MR imaging. Photomicrograph of the surgical specimen showing many strongly HIF1-alpha-positive cells (original magnificationx400) (C). Axial T2-weighted MR image from a 53-year-old female with oligodendroglioma, showing a diffuse infiltrative lesion in the left insulo-operculum (D). [^{18}F]FRP-170 PET image showing no high uptake lesions (E). Photomicrograph showing no HIF1-alpha immunostaining (original magnificationx400) (F).